JOURNAL OF CATALYSIS 89, 545–549 (1984)

Electron Microscopy of β-Bismuth Molybdate

Over the years many research workers have examined mechanisms of oxidation and ammoxidation of hydrocarbons over bismuth molybdates, mainly from the viewpoint of reaction products (e.g. (*1, 2*)). Microstructural changes in the catalysts under reaction conditions, however, greatly influence their selectivity and activity, and investigations of these have been limited.

Detailed solid state chemical work on the Bi–Mo–O system has shown the presence of three active phases, namely, $Bi_2Mo_3O_{12}$ (α-phase), Bi_2MoO_6 (γ-phase), and $Bi_2Mo_2O_9$ (β-phase). Observations of the microstructural changes in the α- and γ-phases by electron microscopy (*3*) and by X-ray photoelectron spectroscopy (*4*) have been reported in the literature. In order to establish a relationship between the microstructure and the reactivity of $Bi_2Mo_2O_9$ (β-phase) we have examined the catalyst by a combination of electron microscopy (EM) methods. EM techniques are ideally suited for the elucidation of the microstructures of powdered catalyst systems which are microcrystalline and often multiphasic.

An AEI-EM7 high-voltage electron microscope (HVEM) fitted with a gas reaction cell was used for direct observations of the surface catalytic reactions. This technique allows the samples to be examined directly under reaction conditions under controlled gas environments at realistic pressures (up to 1 atm) and temperatures (up to ~1000°C) (*3*). Microstructures of the fresh and reacted catalysts were further characterised at higher resolution using the first JEOL JEM 200CX high resolution EM (*5*) at 200 keV which has a point resolution of ~1.7 Å (and a microscope contrast transfer function, CTF, of ~2.4 Å at optimum defocus conditions). Microstructural characterisation was supplemented by local chemical composition analyses by analytical EM (AEM) using the Oxford field emission gun STEM (for crystallites with diameter <100 nm) and by electron probe microanalysis (EPMA) using an automated Cameca microprobe fitted with energy dispersive and wavelength dispersive spectrometers (EDS and WDS). EPMA (WDS) analyses were carried out using well-characterised standards of Bi_2O_3, $Bi_2Mo_2O_9$, and Bi, and concentrations of Bi and Mo in the reacted crystallites were determined by measuring the intensities of M_α and L_α lines for Bi and Mo and the oxygen content in the unit was analysed by difference. Quantitative corrections of the spectra were carried out using the standard MBXCOR programs (for details, see Ref. (*3*)). Parallel experiments on larger (~2 g) amounts of similar samples under conditions identical to those used in the dynamic studies were performed in a fixed-bed microreactor connected to a Varian gas chromatograph–VG mass spectrometer system.

The structure of $Bi_2Mo_2O_9$ is complex; an outline model based on powder X-ray diffraction analysis is given by Van den Elzen and Rieck (*6*). This has recently been refined by Sleight (*7*) based on a single-crystal X-ray diffraction study. According to the latter, the unit cell has $a = 11.972$ Å, $b = 10.813$ Å, $c = 11.898$ Å, $\beta = 90.15°$, with a space group $P2_1/C$ and eight formula units. Bi^{3+} is coordinated to eight oxygens and Mo^{6+} is tetrahedrally coordinated. The cations together with four bismuth vacancies are distributed within the unit cell.

0021-9517/84 $3.00

FIG. 1. SEM image showing morphology of the fresh $Bi_2Mo_2O_9$ catalyst.

Fresh powdered catalyst samples deposited on 2.3-mm copper grids (with a holey carbon film support) were used for electron microscopy. The morphology of the fresh catalyst is illustrated in the scanning electron micrograph (SEM) shown in Fig. 1. Detailed scan of the samples showed that flat crystallites have two major crystallographic projections or likely faces exposed for catalysis, namely (101) and (010) shown in Fig. 2. Other projections observed, though less frequently, were (100), (001), (111), and (112), among others. A structure image of $Bi_2Mo_2O_9$ in (010) projection is shown in Fig. 2c with the simulated image inset. (The image was calculated using the normal multislice methods of the dynamic theory of electron diffraction on a digital image processing Intellect system coupled to the JEM 200CX (*8*). The agreement between the experimental and the calculated image is satisfactory. The high-resolution image in Fig. 2c also shows some contrast anomalies (e.g., those arrowed) indicative of small defect clusters in the fresh material.

The dynamic experiments were carried out in propylene balanced by helium at a pressure of 100 Torr, from room temperature (RT) to ~500°C. At operating temperatures of ~400–440°C, the fresh catalyst

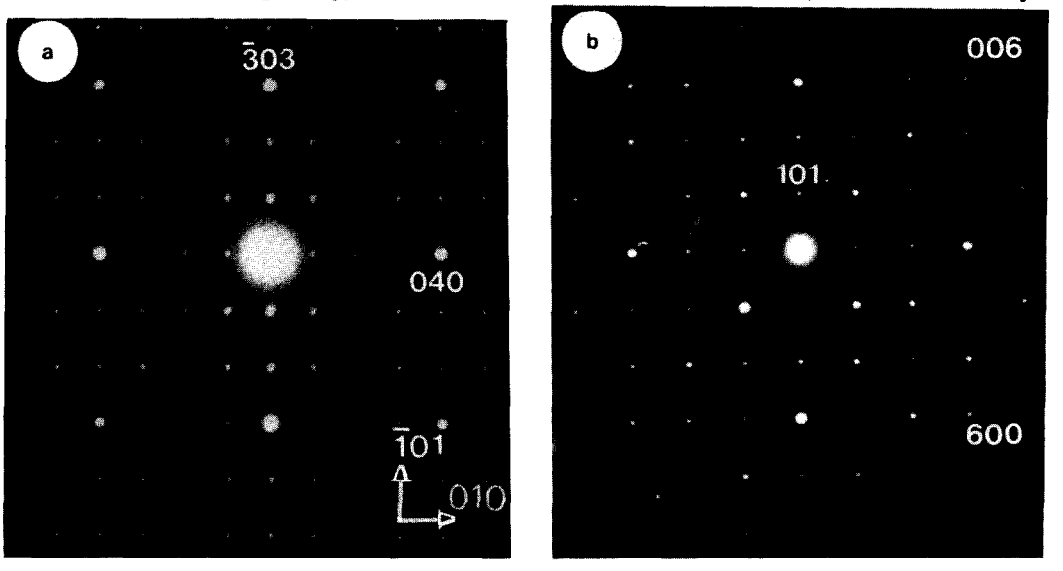

FIG. 2. Two major crystallographic faces observed in the catalyst with some of the reflections indexed: (a) (101) and (b) (010). (c) High-resolution structure image of $Bi_2Mo_2O_9$ in (010) projection with simulated-image inset. Some contrast anomalies are also seen (indicated by arrows), indicative of defect clusters in the fresh catalyst (defocus = −575 Å, 200 kV).

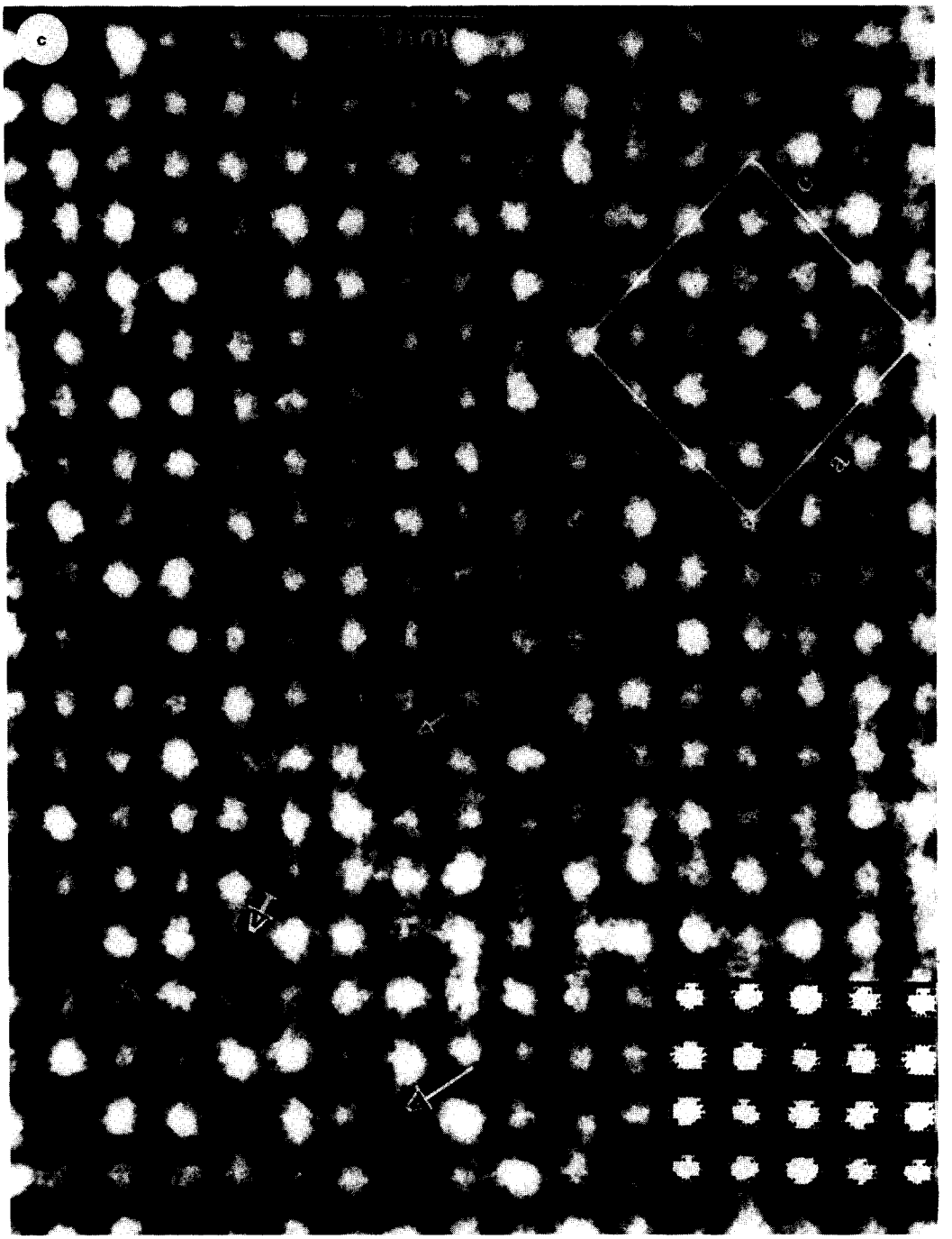

FIG. 2—*Continued.*

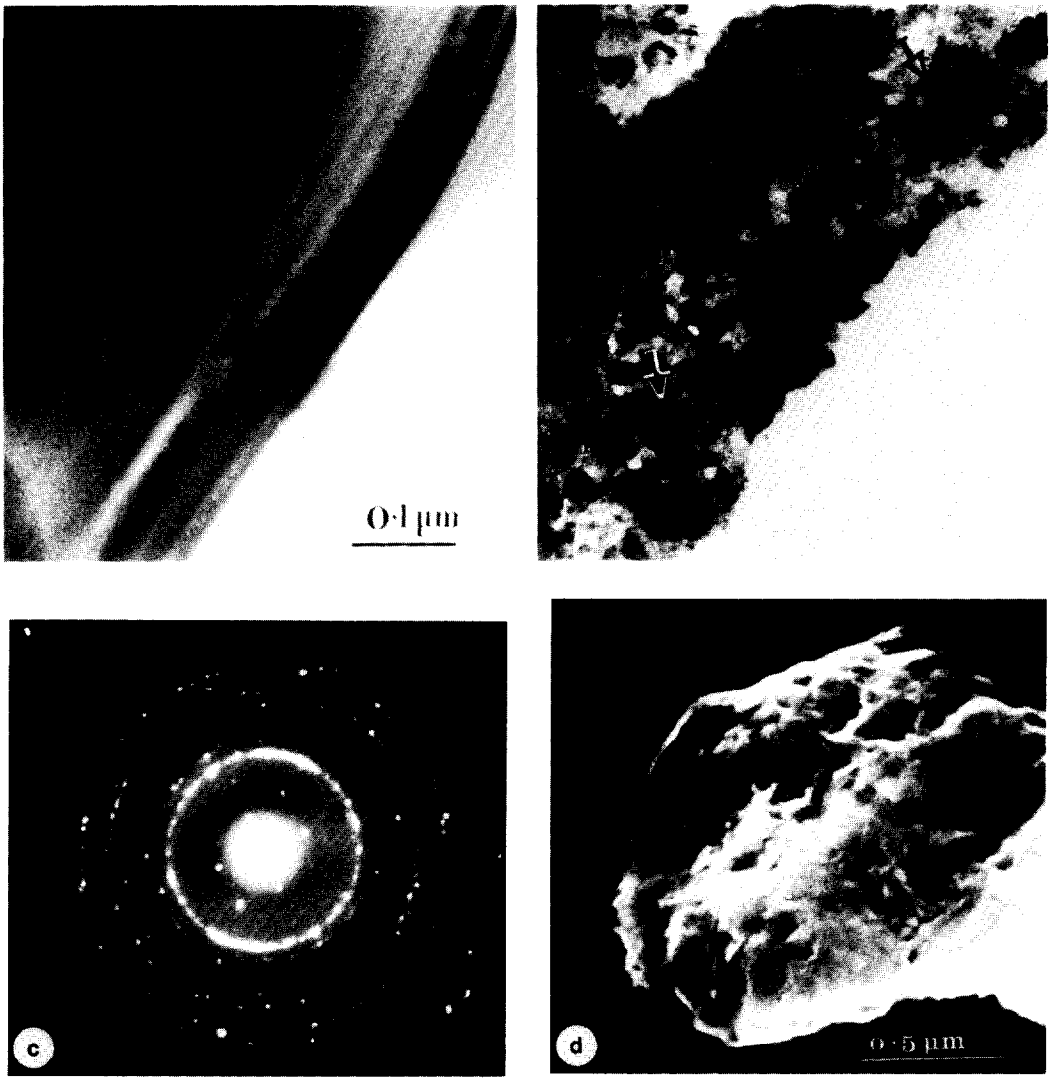

FIG. 3. Reaction of $Bi_2Mo_2O_9$ in C_3H_6 environment: (a) fresh catalyst, (b) decomposition of the catalyst at operating temperature into microcrystalline aggregates, (c) electron diffraction pattern of the reacted material indicating the presence of mostly Bi_2O_3 together with some Bi rings superimposed onto $[11\bar{2}]$ $Bi_2Mo_2O_9$ (host) diffraction pattern. Rings due to Bi_2O_3 are shown at B (e.g., rings 1, 2, 3) and those due to Bi at A. Some rings due to Mo-oxide degradation products can be seen at C. (d) SEM image of the reacted crystallite showing surface roughness.

(Fig. 3a) decomposed into microcrystalline aggregates (Fig. 3b). The selected area electron diffraction patterns recorded for several reacted crystallites showed the presence of Bi_2O_3 as well as Bi, MoO_3, and its degradation products. An example is shown in Fig. 3c; rings due to Bi_2O_3 (for example, at B) and those due to Bi (e.g., at A) are superimposed on the $[11\bar{2}]$ host ($Bi_2Mo_2O_9$) diffraction pattern. SEM images of the reacted crystallites showed considerable surface roughness as indicated in Fig. 3d. The decomposition of the sample into microcrystalline aggregates was the only reaction sequence frequently observed in the reduction experiments at operating tem-

peratures. The presence of Bi_2O_3, some Bi- and Mo-oxides in the reduced material was confirmed by microanalysis using both EDS and WDS. Parallel GC–MS studies and subsequent examination of the reacted samples by EM confirmed the dynamic observations and showed that the selectivity to acrolein decreased as the presence of the degradation products (Bi_2O_3, Bi) increased in the samples. Using gas-phase oxygen in the feed inhibited the disintegration of the samples and prolonged activity.

The observations suggest that the active phase in the reactions is $Bi_2Mo_2O_9$. Pertinent to these findings are the observations of microstructural changes in $Bi_2Mo_3O_{12}$ and Bi_2MoO_6 by *in situ* electron microscopy (*3*) and XPS which have suggested that the selective oxidation of propylene is enhanced due to the presence of the active intermediate $Bi_2Mo_2O_9$ phase. The role of cation vacancies, however, is not clear, but it was suggested that (*9*) they may enhance oxygen mobility. Based on the kinetic and spectroscopic data on doped bismuth molybdates, Bradzil *et al.* (*10*) have now demonstrated that bismuth is responsible for the formation of the allylic intermediate from propylene (constituting the rate-determining step) and the cation vacancies indeed facilitate insertion of oxygen or nitrogen into the intermediate in the selective oxidation/ammoxidation reactions, thus improving oxygen mobility and, therefore, the activity.

ACKNOWLEDGMENTS

The SERC (U.K.) is thanked for financial support. Thanks are also due to Sir Peter Hirsch for the provision of laboratory facilities, and to Dr. A. W. Sleight and Dr. U. Chowdhry of Central Research & Development, DuPont (Delaware) for very useful discussions.

REFERENCES

1. Gates, B. C., Katzer, J. R., and Schuit, G. C. A., "Chemistry of Catalytic Processes." McGraw–Hill, New York, 1979.
2. Hucknall, D. J., "Selective Oxidation of Hydrocarbons." Academic Press, New York, 1974.
3. Gai, P. L., *J. Solid State Chem.* **49,** 25 (1983).
4. Matsuura, I., Schut, R., and Hirakawa, K., *J. Catal.* **63,** 150 (1980).
5. Boyes, E. D., Watanabe, E., Skarnulis, A. J., Hutchison, J. L., Gai, P. L., Jenkins, M. L., and Naruse, M., *Conf. Ser. Inst. Phys. (London),* **52,** Chap. 10, 445 (1980).
6. Van den Elzen, A. F., and Rieck, G. D., *Mater. Res. Bull.* **10,** 1163 (1975).
7. Sleight, A. W., personal communication, 1982.
8. Boyes, E. D., Muggridge, B., and Goringe, M. J., *J. Microsc.* **127,** 321 (1982).
9. Gai, P. L., *in* "Proceedings, 4th International Conference on Chemistry and Uses of Molybdenum" (H. F. Barry and P. C. H. Mitchell, Eds.), p. 296. Climax Molybdenum Company of Michigan, Ann Arbor, Michigan, 1982.
10. Bradzil, J. F., Glaeser, L. C., and Grasselli, R. K., *J. Catal.* **81,** 142 (1983).

P. L. GAI

Department of Metallurgy and Science of Materials
University of Oxford
Parks Road, Oxford OX1 3PH
United Kingdom

Received February 27, 1984